Bioorganic & Medicinal Chemistry Letters 20 (2010) 1801–1815

Contents lists available at ScienceDirect

Bioorganic & Medicinal Chemistry Letters

journal homepage: www.elsevier.com/locate/bmcl

Bioorganic & Medicinal Chemistry Letters Volume 20, Issue 6, 2010

Contents

ARTICLES

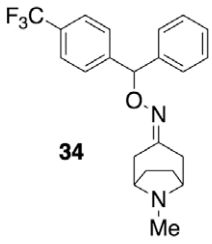

T. cruzi EC_{50} 30nM
Cytotoxicity EC_{50} 35 μM

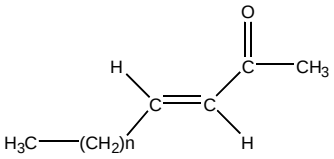

n = 6 to 12

A number of long-chain (*E*)-3-alken-2-one homologues of the naturally occurring antimicrobial compound (*E*)-3-tridecen-2-one were prepared and their antimicrobial activity reported.

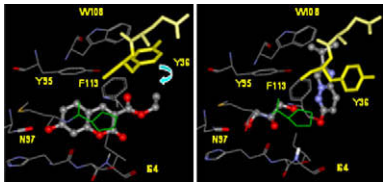

Fragment screening by in silico docking followed by X-ray crystallography demonstrates the formation of a previously unreported surface binding site in MIF that is hydrophobic and surrounded by aromatic side-chain residues.

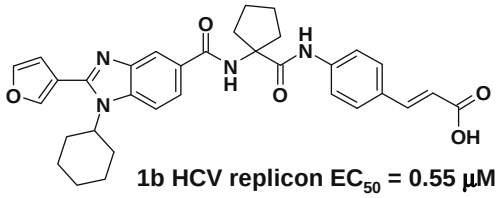

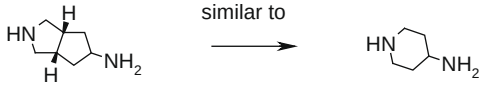

The bicyclic 5-amino-3-azabicyclo[3.3.0]octanes were shown to be effective replacements for the 4-aminopiperidine ring system found in several series of chemokine receptor CCR5 antagonists.

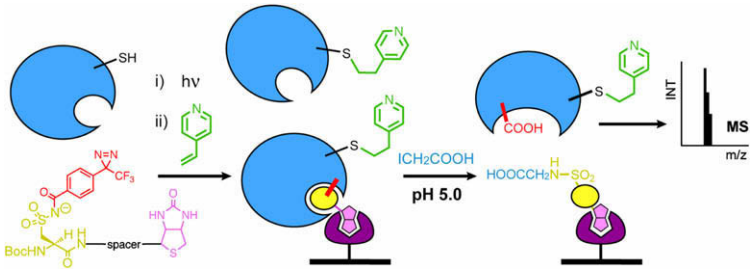

Highly efficient profiling of labeled peptide was achieved with cleavable biotinylated probe by utilizing selective S- and N-alkylation.

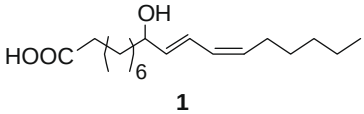

1

As an unprecedented NES non-antagonistic inhibitor for nuclear export of Rev, (10*E*,12*Z*)-9-hydroxyoctadeca-10,12-dienoic acid (**1**) was disclosed. Additionally, structure–activity relationship analysis clarified cooperation of several functionalities in potency of **1**.

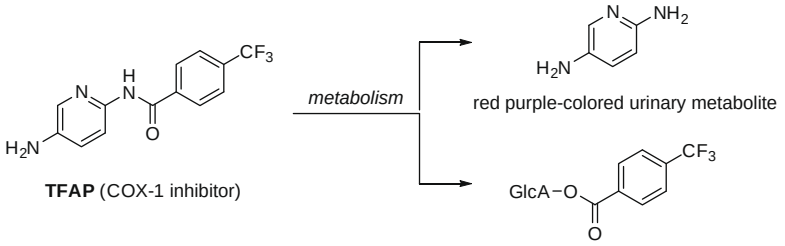

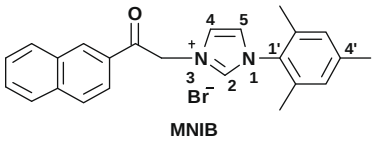

An imidazolium salt, 1-mesityl-3-(2-naphthoylmethano)-1*H*-imidazolium bromide (MNIB), has been investigated for its antitumor properties. In vitro studies demonstrate that MNIB is active against K562, SMMC-7721, EJ, AGZY, HEP-2, A549, HepG2, and Raji tumor cells, and can induce the G1 phase cell cycle arrest and apoptosis in K562 cells. Moreover, administration of MNIB significantly inhibited tumor growth in human non-small lung tumor (A549) xenografts.

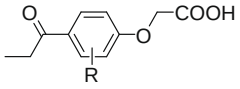

Analogues of ethacrynic acid, lacking the α,β-unsaturated carbonyl unit, were designed, synthesized, and subsequently evaluated for their cytotoxicity and anti-migratory effects against human MCF-7/AZ breast cancer cells.

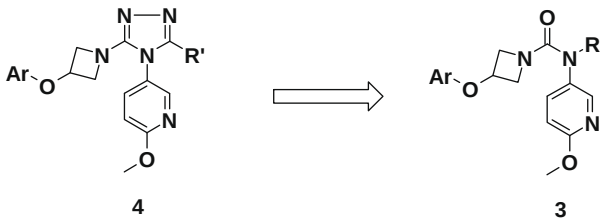

A series of azetidine ureas, **3**, were prepared as potential bioisosteres of previously reported azetidinyltriazole oxytocin antagonists, **4**. Several potent analogues were prepared and one, compound, **9**, demonstrated significant levels of selectivity over the closely related vasopressin V_{1A} receptor.

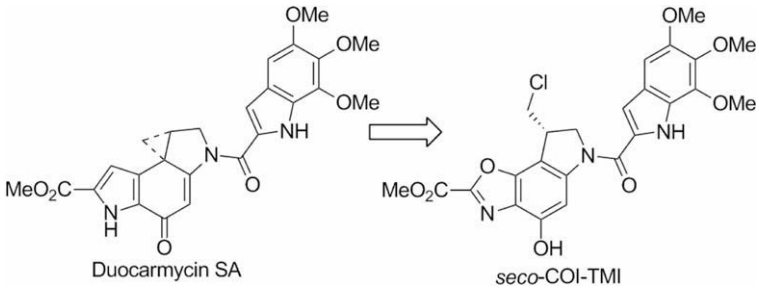

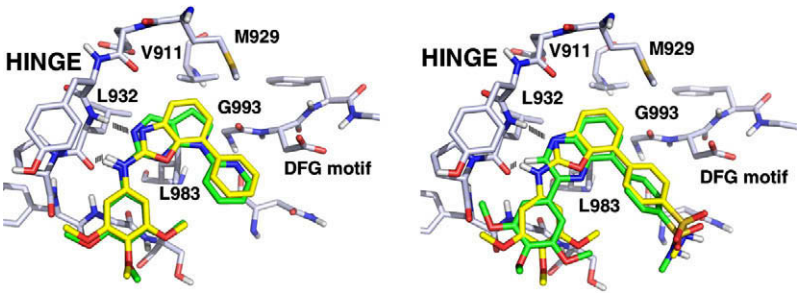

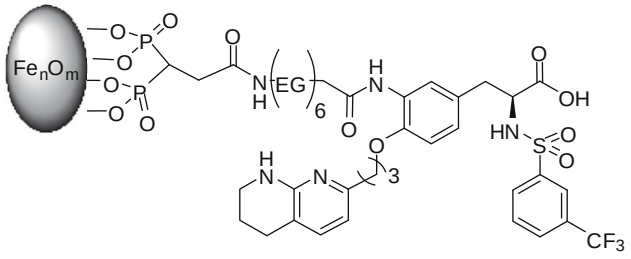

USPIO–peptidomimetic conjugate targeting Jurkat cells.

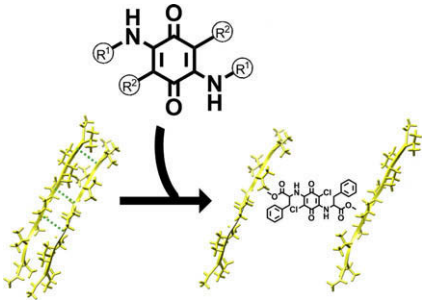

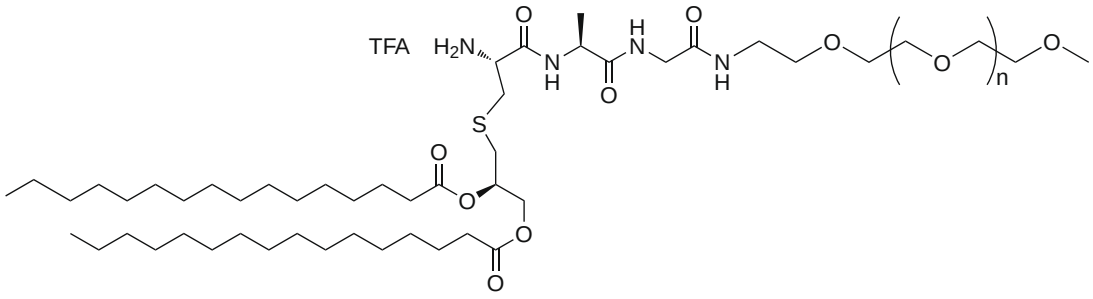

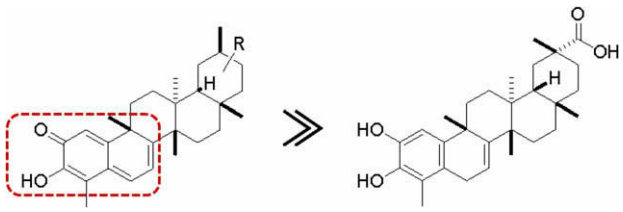

The presence of a quinone-methide moiety appears to play a relatively significant role in 3CL^{pro} inhibition.

A novel series of hydantoin TACE inhibitors is disclosed. The initial design and SAR optimization of the series, as well as accompanying X-ray structural and modeling considerations, are described.

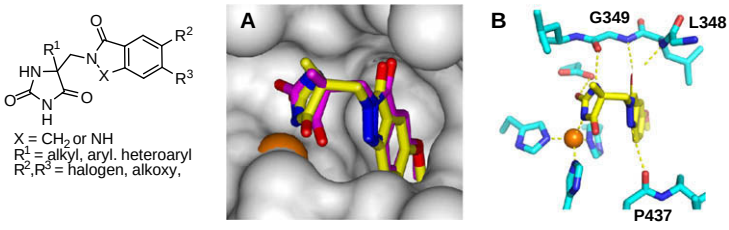

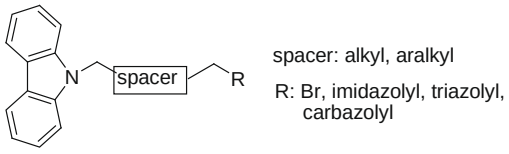

A series of carbazole derivatives were synthesized and evaluated for antibacterial and antifungal activities.

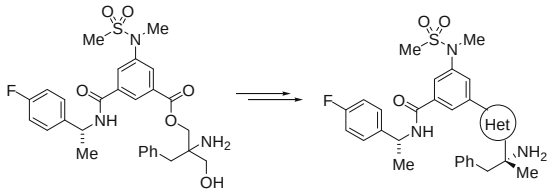

This Letter describes SAR of the tertiary carbinamine derived inhibitors of BACE1 revealed during the optimization of the unstable lead toward potent and stable heterocycle linked compounds. The incorporation of a flap interaction with the target enzyme was not critical for potency. A trend observed during this optimization was that the pK_a of the amine derived aspartate ligand needed to be at least close to that of the assay medium for BACE1 inhibition.

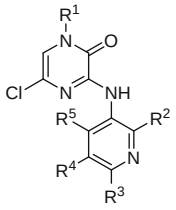

The structure–activity relationships of a series of N^3-pyridylpyrazinones as corticotropin-releasing factor-1 receptor antagonists was investigated.

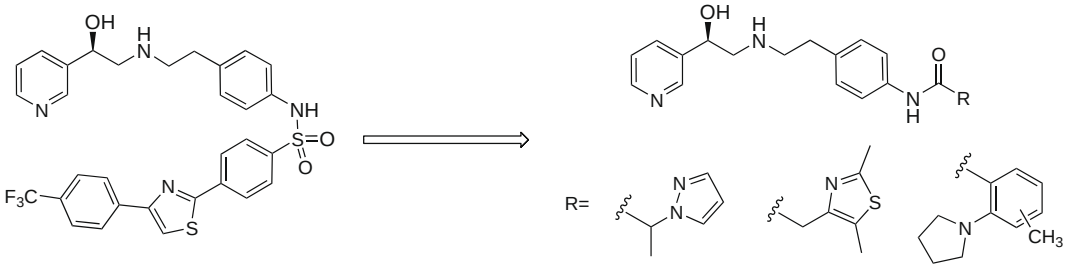

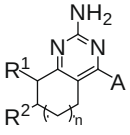

Three novel series of histamine H_4 receptor (H_4R) antagonists containing the 2-aminopyrimidine motif are reported.

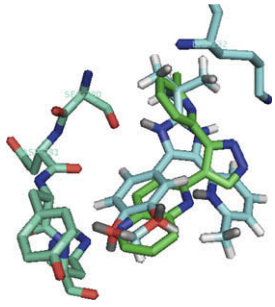

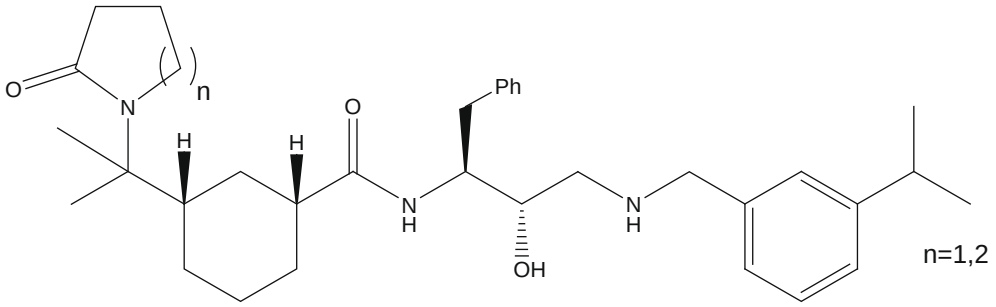

Compounds	Dosage (mg/kg)	PT (4 d)	PT (10 d)	VII% (4 d)	VII% (10 d)	X% (4 d)	X% (10 d)
Control	0	12.8	12.9	400.0	321.3	60.6	58.1
warfarin (**1**)	0.25	37.0	24.4	29.5	56.2	10.0	14.9
1 + 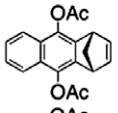	0.25 + 2.5	40.5	35.4	20.3	35.0	4.8	7.7
1 + 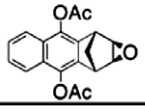	0.25 + 2.5	12.0	108.4	264.0	18.4	58.8	3.6

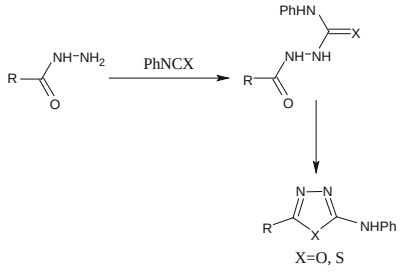

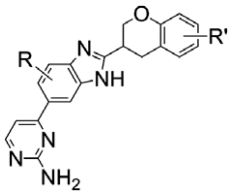

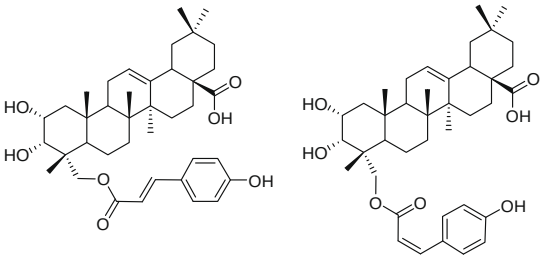

A bioassay-guided fractionation and chemical investigation of the trunk of *Berberis koreana* resulted in the isolation and characterization of two new triterpenoids (**1**–**2**), along with seven known triterpenoids (**3**–**9**).

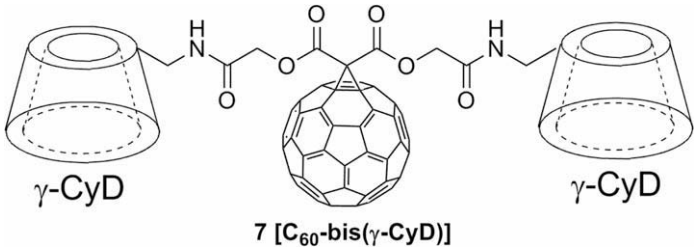

Syntheses of water-soluble C_{60} derivatives and the examination of their enhancing effect on neurite outgrowth of NGF-treated PC12 cells are reported.

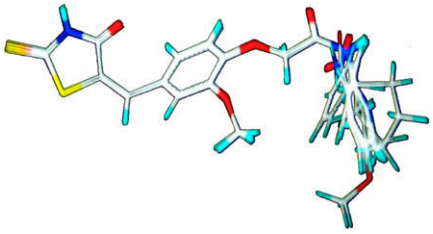

Designed, synthesized, and evaluated some novel glitazones for their antidiabetic activity.

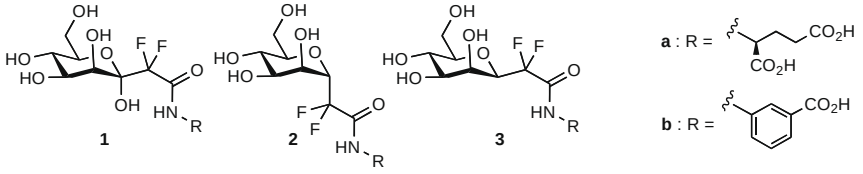

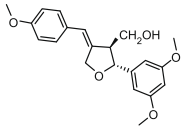

2a

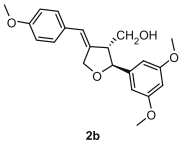

2b

Two chiral furan lignan was synthesized, chiral separated and their absolute configuration was determined by circular dichroism spectra. Compound **2c** (IC_{50} = 12 μM on QGY-7701), the racemate of **2a** and **2b**, is reported.

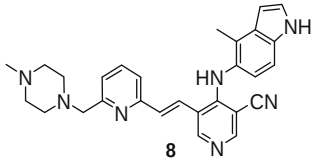

8

The 3-pyridinecarbonitrile **8** has an IC_{50} value of 1.1 nM for the inhibition of PKCθ and blocks the production of IL-2 in both stimulated murine T cells (IC_{50} = 34 nM) and human whole blood (IC_{50} = 500 nM).

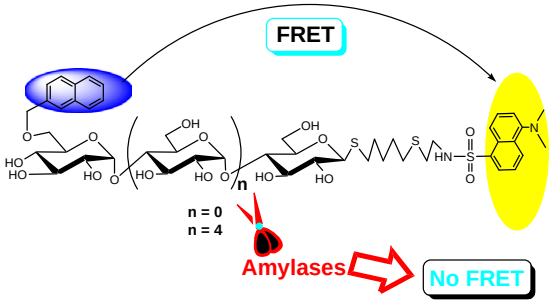

This Letter describes a chemical lead optimization campaign directed around VU0119498, a pan G_q mAChR M_1, M_3, M_5 PAM, which previously afforded the first selective M_5 PAM. An iterative library synthesis approach delivered a novel chemotype with selective M_1 PAM activity (no activity at M_2–M_5 @ 30 μM), and comparable M_1 potency (EC_{50} = 830 nM) to the prototypical M_1 PAM, BQCA.

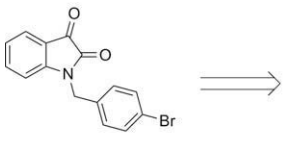

VU0119498 (**1**)

M_1 EC_{50} = 6.1 μM
M_2 EC_{50} >30 μM
M_3 EC_{50} = 6.4 μM
M_4 EC_{50} >30 μM
M_5 EC_{50} = 4.1 μM

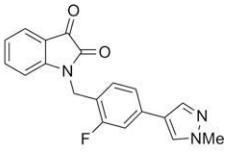

VU0366369 (**12a**)

M_1 EC_{50} = 0.83 μM
M_2 EC_{50} >30 μM
M_3 EC_{50} >30 μM
M_4 EC_{50} >30 μM
M_5 EC_{50} >30 μM

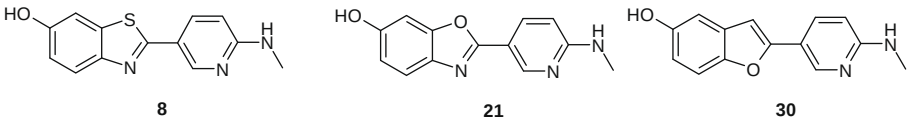

8 **21** **30**

The syntheses and SAR of new series of β-amyloid binding agents are reported. The effort to optimize signal-to-background ratios for these ligands are described. Compounds **8, 21** and **30** displayed desirable lipophilicity and pharmacokinetic properties. Compounds **8** and **21** were evaluated with in vitro autoradiographic studies and in vivo in APP/PS1 transgenic mice. It is shown that it was possible to increase the signal-to-background ratios compared to PIB **1**, as demonstrated by compounds **8** and **21**.

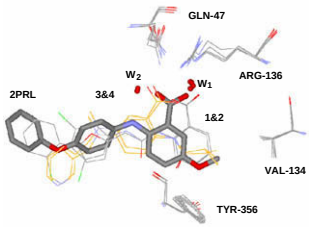

Several amino-benzoic acid derivatives were found to be DHODH inhibitors through virtual screening, biochemical, and X-ray crystallographic studies.

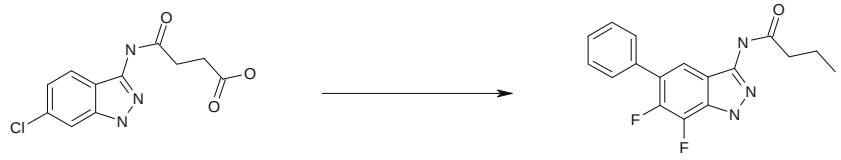

GSK3 β IC_{50} = 1.18 μM

GSK3 β IC_{50} = 6 nM
Cdk1 IC_{50} = 2.5 μM
Cdk2 IC_{50} = 3.2 μM

From an HTS hit, a series of potent and selective inhibitors of GSK3β have been designed based on a Cdk2-homology model and with the help of several crystal structures of the compounds within Cdk2.

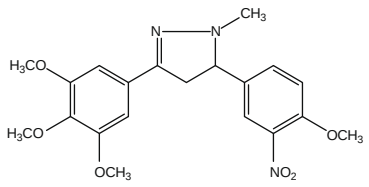

IC_{50} 0.213 mM

The synthesis and the ACE inhibitory activity of chalcones (**1**–**9**) and pyrazoles (**10**–**18**) are reported.

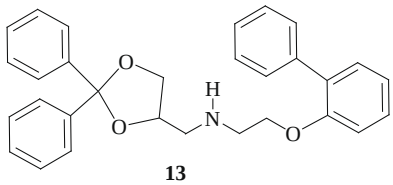

13

A new series of 5-HT_{1A} receptor agonists has been discovered. Compound **13**, which combines high selectivity (5-HT_{1A}/α_1 = 151) and good agonist potency (pD_2 = 7.82; E_{max} = 76), was found to be the most interesting of the series.

A new bisindole alkaloid, bisleuconothine A (**1**) consisting of an eburnane–aspidosperma type skeleton, was isolated from the bark of *Leuconotis griffithii*. The structure including absolute stereochemistry was elucidated on the basis of 2D NMR data and X-ray analysis. Bisleuconothine A (**1**) showed cell growth inhibitory activity against various human cancer cell lines.

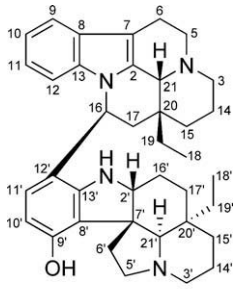

1

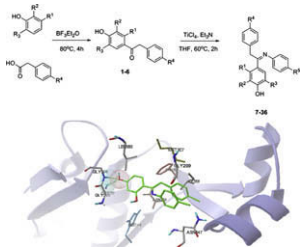

A novel series of deoxybenzoin derivatives were designed and synthesized. Based on the biological data obtained in this study, it can be concluded that compound **19** would be a potential *Escherichia coli* FabH inhibitor and promising anti-inflammatory agent. The binding model of compound **19** and *E. coli* FabH was also been researched.

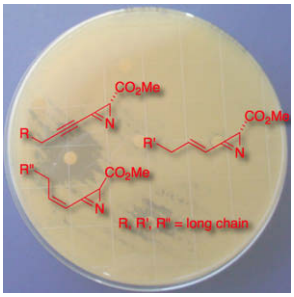

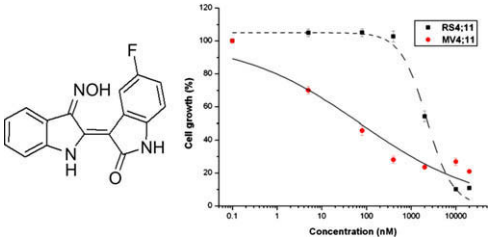

5-Fluoro-indirubin-3′-oxime, **13** exhibited potent inhibitory activity at FLT3 (IC_{50} = 15 nM) with more than 100-fold selectivity versus 6 other kinases and potent anti-proliferative effect for MV4;11 cells (IC_{50} = 72 nM) with 30-fold selectivity versus RS4;11 cells.

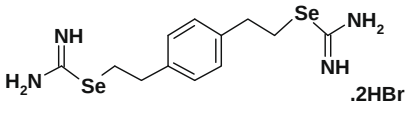

PBISe

Our studies demonstrate that substitution of sulfur with selenium in known iNOS inhibitor increases the compound's potency by several folds in variety of different cancers cell lines tested. Hence, this approach may be used as a strategy to increase the efficacy of the anticancer agents.

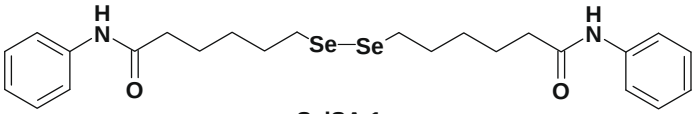

SelSA-1

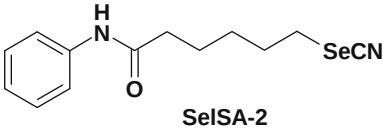

SelSA-2

In order to develop novel HDAC inhibitors, two selenium analogs modeled after SAHA were synthesized and found to be highly potent HDAC inhibitors having IC_{50} values in low nanomolar range.

*Corresponding author
Supplementary data available via ScienceDirect

COVER

Overlay of high resolution co-crystal structures of *R*-**22**-ADP (cyan) and **1**-ADP (green) bound in an allosteric binding site of the mitotic kinesin KSP. [Roecker, A. J.; Coleman, P. J.; Mercer, S. P.; Schreier, J. D.; Buser, C. A.; Walsh, E. S.; Hamilton, K.; Lobell, R. B.; Tao, W.; Diehl, R. E.; South, V. J.; Davide, J. P.; Kohl, N. E.; Yan, Y.; Kuo, L. C.; Li, C.; Fernandez-Metzler, C.; Mahan, E. A.; Prueksaritanont, T.; Hartman, G. D. *Bioorg. Med. Chem. Lett.* **2007**, *17*, 5677.]

Indexed/Abstracted in: Beilstein, Biochemistry & Biophysics Citation Index, CANCERLIT, Chemical Abstracts, Chemistry Citation Index, Current Awareness in Biological Sciences/BIOBASE, Current Contents: Life Sciences, EMBASE/Excerpta Medica, MEDLINE, PASCAL, Research Alert, Science Citation Index, SciSearch, TOXFILE. Also covered in the abstract and citation database SCOPUS®. Full text available on ScienceDirect®

ELSEVIER

ISSN 0960-894X